

# Tuning Light Emission of a Pressure-Sensitive Silicon/ZnO Nanowires Heterostructure Matrix through Piezo-phototronic Effects

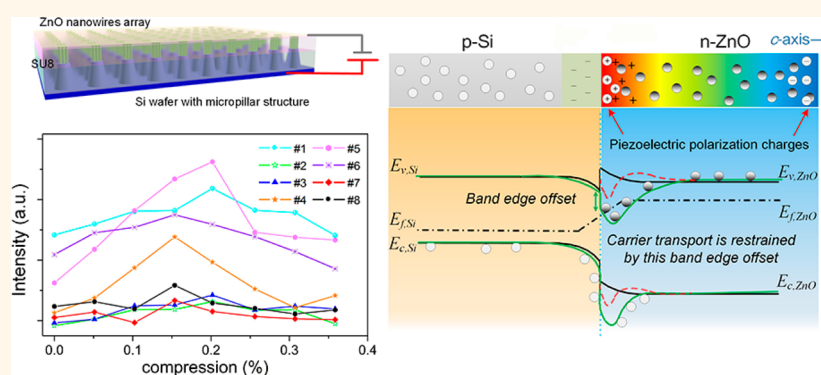
Mengxiao Chen,<sup>†</sup> Caofeng Pan,<sup>\*,†</sup> Taiping Zhang,<sup>†</sup> Xiaoyi Li,<sup>†</sup> Renrong Liang,<sup>‡</sup> and Zhong Lin Wang<sup>\*,†,§</sup>

<sup>†</sup>Beijing Institute of Nanoenergy and Nanosystems, Chinese Academy of Sciences; National Center for Nanoscience and Technology, Beijing 100083, P. R. China

<sup>‡</sup>Institute of Microelectronics, Tsinghua University, Beijing 100084, P.R. China

<sup>§</sup>School of Materials Science and Engineering, Georgia Institute of Technology, Atlanta, Georgia 30332-0245, United States

## Supporting Information



**ABSTRACT:** Based on white light emission at silicon (Si)/ZnO heterojunction, a pressure-sensitive Si/ZnO nanowires heterostructure matrix light emitting diode (LED) array is developed. The light emission intensity of a single heterostructure LED is tuned by external strain: when the applied stress keeps increasing, the emission intensity first increases and then decreases with a maximum value at a compressive strain of 0.15–0.2%. This result is attributed to the piezo-phototronic effect, which can efficiently modulate the LED emission intensity by utilizing the strain-induced piezo-polarization charges. It could tune the energy band diagrams at the junction area and regulate the optoelectronic processes such as charge carriers generation, separation, recombination, and transport. This study achieves tuning silicon based devices through piezo-phototronic effect.

**KEYWORDS:** piezo-phototronic effect, heterojunction LED, pressure sensitive, nanowire matrix, light emission modulation

Extensive investigations in piezotronic and piezo-phototronic effects have been carried out in both theoretical analysis and device applications.<sup>1–3</sup> There are many excellent works involving traditional piezoelectric materials, such as ZnO,<sup>4–6</sup> GaN, CdS,<sup>7</sup> and so on. Their outstanding performance in transmissions between mechanical agitations and electronic signals has contributed to applications including pressure mapping,<sup>4</sup> electrical skin,<sup>8,9</sup> and other human-machine interface engineering. However, it is challenging to interface mechanical stimuli with the advanced Si-based technology directly. The indirect bandgap structure of Si makes it difficult for carrier recombination and photon generation. A heterostructured Si-piezoelectric material system has been proposed as a promising solution. Photodetection<sup>10</sup> and white light emission have been achieved in this structure through p-porous Si/ZnO heterojunction. Thus, the Si/ZnO system could be

considered as a candidate for a pressure-sensitive photoelectric device,<sup>11</sup> as ZnO is a traditional piezoelectric material sensitive to mechanical stimulations.<sup>12</sup> The disordered topography of porous Si limits the potential application in modern human-machine interface optoelectronics. We therefore developed a regular pixelated Si/ZnO heterojunction structured device to utilize the pressure sensitivity advantage of ZnO and the mature fabrication procedures of Si. This optoelectronic device works as a pressure-sensitive LED matrix and is expected to be applied in pressure electroluminescence mapping, optical communication, integrated optical circuits, and so on.

Received: March 8, 2016

Accepted: June 8, 2016

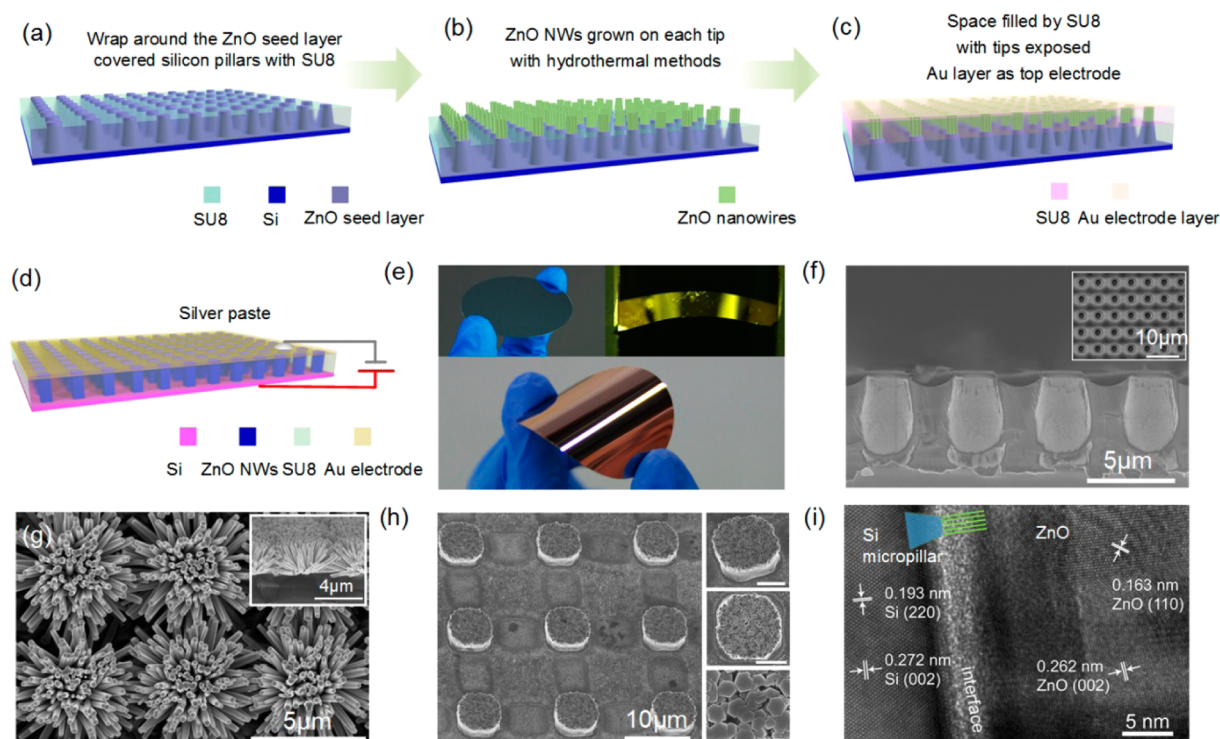


**Figure 1.** Device fabrication. (a–c) Schematic diagrams illustrating the fabrication process of the Si micropillar/ZnO nanowires heterostructure matrix (SZHM) LED (fabricated on microstructured silicon wafers). (d) Structure design of the SZHM device fabricated on a flat (nonstructured) p-Si wafer. (e) The SZHM device fabricated on flexible silicon wafer (the upright figure is the integrated device fixed on the test stage). (f) SEM image of the silicon pillar array after depositing a ZnO seed layer and wrapping around them with SU8. The tips were exposed after oxygen plasma etching. (g) As-grown ZnO nanowires on the top of the tip array through low temperature hydrothermal methods. (h) ZnO nanowires array grown on nonstructured p-Si wafers through photolithography and low temperature hydrothermal method. The pixel size was set as  $5\ \mu\text{m}$  through lithography fabrication. The scale bars are  $3\ \mu\text{m}$ ,  $3\ \mu\text{m}$ , and  $500\ \text{nm}$ , respectively, from the top to the bottom. (i) TEM image showing the interface between silicon and ZnO layers, indicating the (001) direction of ZnO nanowire is perpendicular to the ZnO/Si interface [001].

In this work, the optoelectronic device is developed as a pressure-sensitive Si/ZnO nanowires heterostructure matrix (SZHM) LED. The ZnO nanowire-bunched matrixes were fabricated on both micropillar array structured and nonstructured silicon wafers. Besides white light emission, precise pressure based light intensity control is achieved in the Si/ZnO material system. The light emission intensity of a single LED ( $2.5\ \mu\text{m}$ , a Si micropillar/ZnO nanowires heterojunction contact) in the SZHM increases with applied stress until a maximum value is reached at a compressive strain of 0.15%–0.2%, and then it decreases. This result is attributed to the piezo-phototronic effect,<sup>13–17</sup> which can efficiently modulate the light emission intensity of LEDs by utilizing the strain induced piezo-polarization charges created at the interface, which tune the energy band diagrams and the optoelectronic processes such as charge-carrier generation, separation, recombination, and transport. Furthermore, this observation verified the piezo-phototronic energy band modulation theory.<sup>3</sup> It provides a promising method to manipulate the light emissions of LEDs based on piezoelectric semiconductors by the piezo-phototronic effect through applying static strains and may find perspective applications in various optoelectronic devices<sup>18</sup> and integrated systems.

## RESULTS AND DISCUSSION

The fabrication process of the pressure-sensitive SZHM LED array is illustrated in Figure 1. P-type Si wafers ( $\rho \approx 0.01\ \Omega\cdot\text{cm}$ )

were used to fabricate the micropillar structures through a photolithography method and inductively coupled plasma (ICP) etching. Detailed procedures can be found in the Methods. Parts a–c of Figure 1 illustrates a brief fabrication process of the SZHM LED array on the micropillar structure. A ZnO seed layer was deposited on the as-prepared Si micropillar structure surface by magnetron sputter. In order to make sure the ZnO nanowires only grow on the top of the Si micropillars, SU8 photoresist was spin-coated to fill the space among the Si micropillars. The tips of the Si micropillars are exposed after oxygen plasma etching. Low temperature hydrothermal methods were employed to grow the ZnO nanowires on the top of the tip matrix. To make sure the heterojunction LEDs are uniform, another SU8 layer was used to wrap around the nanowire bunches. All of the tips of vertical grown nanowires were exposed after plasma etching, and an Au electrode layer was deposited on the top as the common top electrode. The bottom electrode was fabricated by adding a silver paste layer on the Si bottom side, and the SZHM device on the micropillar structured substrate was finished. In order to simplify the processing steps, we also attempted to fabricate SZHM directly on nonstructured silicon wafers. A sketch for SZHM fabricated on nonstructured p-silicon wafers is shown in Figure S1. This structure design makes flexible device feasible if it is fabricated on flexible silicon wafer (Figure 1e). Parts f–h of Figure 1 are SEM scanning electron microscopy (SEM) images showing details of

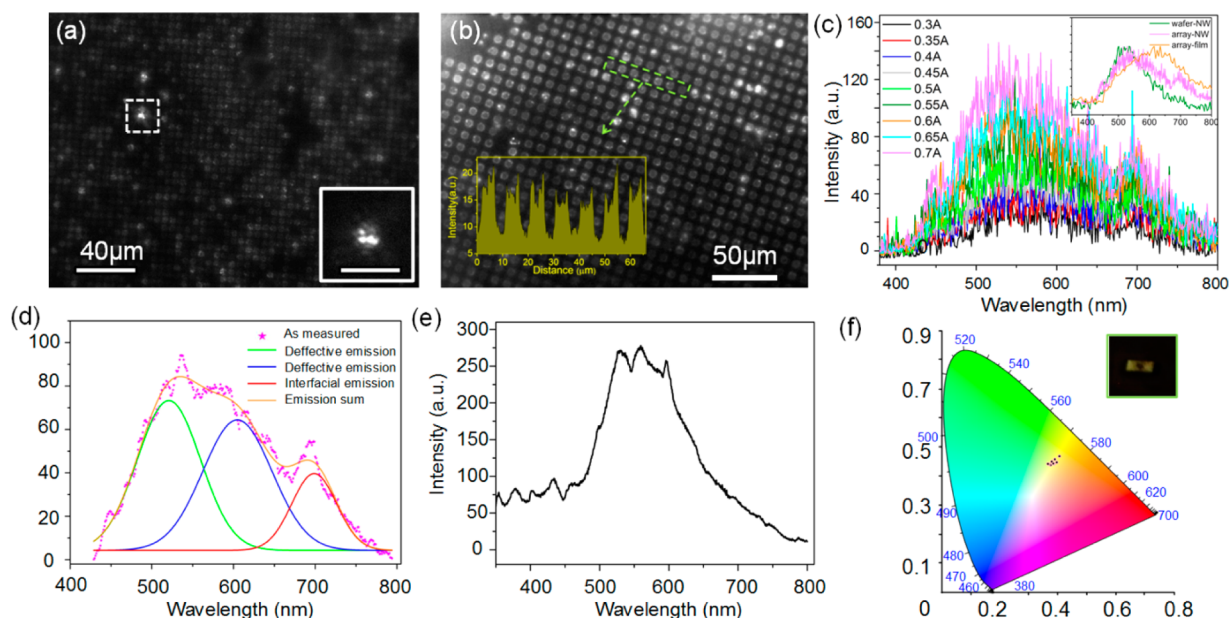


**Figure 2.** Optical properties of the SZHM LED. (a) CCD images under the microscope of the turned on device fabricated on the micropillar structure, and each LED could be easily distinguished. The enlarged insert indicates that the light in a certain LED comes from the independent nanowires, and the scale bar here is  $5 \mu\text{m}$ . (b) CCD images under the microscope of the device fabricated on nonstructured p-Si wafer when electrically emitting light. It shows a more uniform distribution than the pillar array-NWs LED. (c) Electroluminescence spectra as a function of the forward biased current with the inset comparing electroluminescence of three kinds of Si/ZnO white light LEDs: nonstructured p-silicon wafer/n-ZnO nanowires array device, p-silicon micropillar array/ZnO NWs, and p-silicon micropillar array/ZnO nanofilm device. (d) Gauss deconvolution analysis of the white light emission spectra could be decomposed into three distinct emission bands which correspond to three optoelectronic processes (spectrum from Figure 2c when the inject current is 0.6A). (e) Photoluminescence spectrum under a 325 nm laser excitation. (f) The chromaticity diagram shows the white-light LED in the CIE color coordinates. Inset: optical image of a lit-up device.

the SZHM structures. Top and sectional view images in Figure 1f indicate that the height of the micropillar is  $5 \mu\text{m}$  with a  $2.5 \mu\text{m}$  top diameter, and the tips are thoroughly exposed. The average length of the *c*-direction nanowires is  $3 \mu\text{m}$ , and they grow in bunches with only the centric ones upright (Figure 1g) due to the absence of a binding force when growing in the solution. The as grown ZnO pixels on nonstructured silicon wafers were carefully characterized as shown in Figure 1h, and the heterojunction/pixel size was set as  $5 \mu\text{m}$  through lithography mask fabrication. The Si–ZnO interface was characterized by high-resolution transmission electron microscopy (TEM), and the image in Figure 1i indicates that the (001) direction of ZnO nanowire is perpendicular to the ZnO/Si interface [001].

Optical performances of the SZHM LED array are presented in Figure 2. Figure 2a shows the light-emitting performance of the matrix on the micropillar structure, and each LED could be easily distinguished. The inset is the enlarged CCD image of a single LED, from which we can identify that the light in a certain LED comes from each single nanowire, while  $5 \mu\text{m}$  ZnO nanowire bunches on the nonstructured silicon wafer show a more uniform distribution than the “pillar array-NWs” matrix LED (Figure 2b). Emission spectra of the as-fabricated LED were monitored at different biased injected currents at room temperature. The light emission intensity was in positive correlation with injected currents as the electroluminescence spectra shown in Figure 2c, which is in accord with basic semiconductor theories. The inset compares electroluminescence of three different Si/ZnO white light matrix LEDs: p-Si wafer/n-ZnO nanowires matrix device, p-Si micropillar array/ZnO NWs device, and p-Si micropillar array/n-ZnO nanofilm

device. Though differing in details, all of the light emissions mainly come from recombination at the interface and defects in ZnO (spectra from 400 to 700 nm).<sup>19</sup> In order to get further understanding of it, peak deconvolution with Gauss functions was used to analyze the spectra from Figure 2c. Figure 2d indicates that the broad spectrum consists of three distinct bands in the range of 450–580, 500–700, and 650–760 nm, respectively, and each emission band corresponds to a particular recombination process. The green emission band centered at around 520 nm comes from recombination at the dislocation defects energy level of Zn and O in ZnO nanowires.<sup>20</sup> Whereas the red emission band centered at about 600 nm is attributed to the transitions from the conduction band or shallow donor levels to O vacancy energy level in ZnO nanowires.<sup>20,21</sup> The near-infrared emission around 700 nm is ascribed to the radiative interfacial recombination<sup>22</sup> of the holes from p-Si and electrons from n-ZnO.<sup>23</sup> We also measured photoluminescence experiments under a 325 nm laser excitation, and the similar spectral range was observed. To get a visualized performance, the chromaticity diagram (Figure 2f) was used to show the white-light LED in the CIE color coordinates under forward biased voltages. The inset shows the corresponding optical image when the device was lit up in the dark environment with the emission tending to be light yellow color.

As the uniform white light emission has been achieved on this SZHM LED array, it is feasible to tune light intensity by applying pressure on ZnO nanowires by a piezo-phototronic effect. Each Si/ZnO nanowires heterostructure in the matrix could be regarded as a single LED; therefore, we can investigate the pressure modulation process by observing LED light

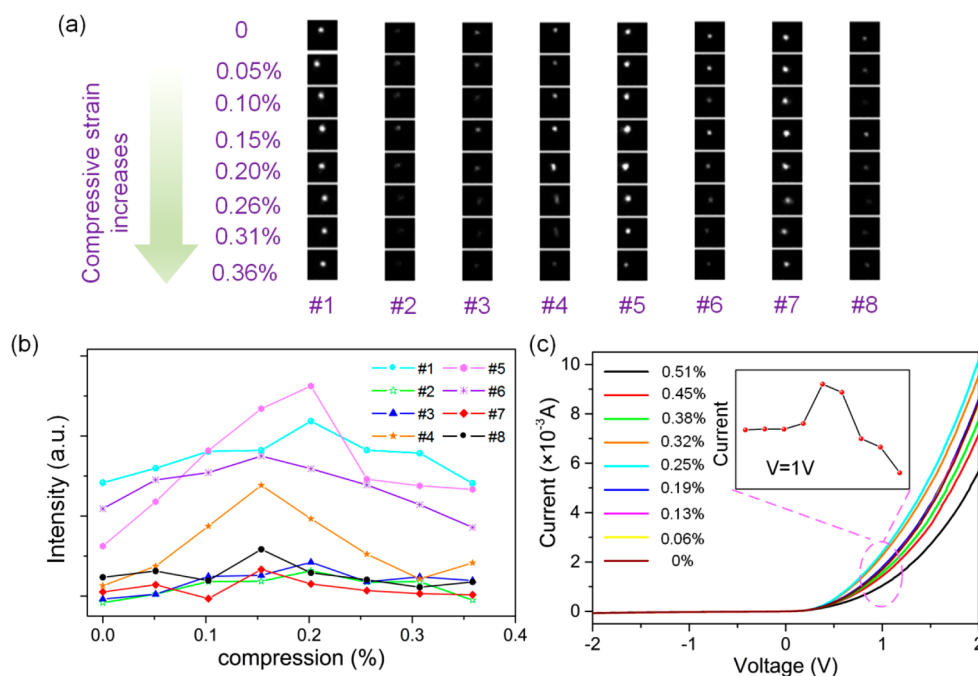


**Figure 3.** Piezo-phototronic effect on the SZHM LED. (a) Light intensity changes under increasing compressive strains shown by CCD images for eight single LEDs, and each number (1–8) stands for one heterojunction LED. (b) Light intensity changes under increasing compressive strains demonstrated by calculated intensities for eight single LEDs in (a), which clearly shows there is a peak value in the piezo-phototronic effect modulating process. (c)  $I$ – $V$  characteristics of the device operated under external strains, with a similar regulating performance with results showing in (a) and (b). The inset indicates that at +1 V applied voltage the current values corresponding to compressions from 0 to 0.51% show a similar trend with the light intensity performance.

intensity. In Figures 3a,b, we present eight LEDs to show their performance while the applied stress is increased. Figure 3a shows that the light intensities of the LEDs were enhanced until the compressive strain reached 0.15%–0.2%, and then they decreased. In order to get a quantificational view, the gray level values for LEDs in eight corresponding rows in Figure 3a, which represents the changing process, were extracted and demonstrated in Figure 3b. We can also find that the maximum value of light intensity appears in a compressive strain range of 0.15%–0.2%. To confirm this phenomenon,  $I$ – $V$  characteristics of the integrated device under different pressure were investigated in Figure 3c. It is clear to conclude that, at the same biased voltage, there is a maximum current value with the externally applied compressive strains, indicating a similar piezo-phototronic effect modulation process<sup>10</sup> as the light emission performances show in Figure 3a,b.

To illustrate the modulation principle, band diagrams of the p-Si micropillars/n-ZnO heterojunction LED devices without biased voltage (Figure 4a), with external compressive strain under forward biased voltage (Figure 4b), and energy band diagrams when the stress increases (Figure 4c) are shown. The bandgap of the microstructured p-Si is 2 eV according to porous silicon theory,<sup>19,22,24</sup> and the bandgap of ZnO is 3.37 eV, so there is conduction band edge offset  $\Delta E_c$  and valence band edge offset  $\Delta E_v$ . When compressive strains are applied along the  $c$ -axis of ZnO, positive piezoelectric polarization charges are induced within the depletion zone, resulting in temporarily trapping of electrons at the interface and band edge downward bending at ZnO side. The conduction band edge offset (n-ZnO side is higher than p-Si side) decreases, and a dip in the local band structure near the interface is created in the p–n junction area (the red line in Figure 4b). The hole concentration in the B-doped p-Si wafer ( $p \sim 10^{18} \text{cm}^{-3}$ ) is

higher than the electron concentration in the n-ZnO nanowire ( $n \sim 10^{17} \text{cm}^{-3}$ ), so the carrier transport is mainly determined by the local density of electrons and their mobility. The decrease of the ZnO conduction band edge at the interface will help the electrons transport to the interface, and the dip could trap more electrons at the interface, increasing the carrier recombination rate and number of photons generated through radiative transition at the interface. However, when the conduction band edge of ZnO decreases to a level that the edges of both p-side and n-side are aligned, the enhancement reaches a peak. If the compressive strain continues increasing, the conduction band edge offset (p-Si side is higher than n-ZnO side) will hamper the electron transportation; thus, the recombination and light emitting are decreased/restrained (Figure 4c), as observed experimentally in Figure 3. At the same time, the transport of holes in this case may start to drastically slow down, and thus the recombination rate drops. This special performance gives a better understanding of piezo-phototronic effect modulated carrier transportation in p–n junctions.<sup>4,25</sup> It also makes the precise pressure-control on light intensity achievable in the Si/ZnO material system, expanding potential applications of Si/ZnO heterojunction LED, e.g., pressure mapping.

## CONCLUSION

In summary, we developed a pressure-sensitive SZHM LED. Besides white light emission, precise light intensity control by pressure is achieved in the Si/ZnO material system. With increased applied stress, the emission intensity first increases and then decreases with a maximum value at a compressive strain of 0.15–0.2%. This special performance is attributed to piezo-phototronic effect. The size of each heterojunction LED is controllable with the help of modern silicon fabrication

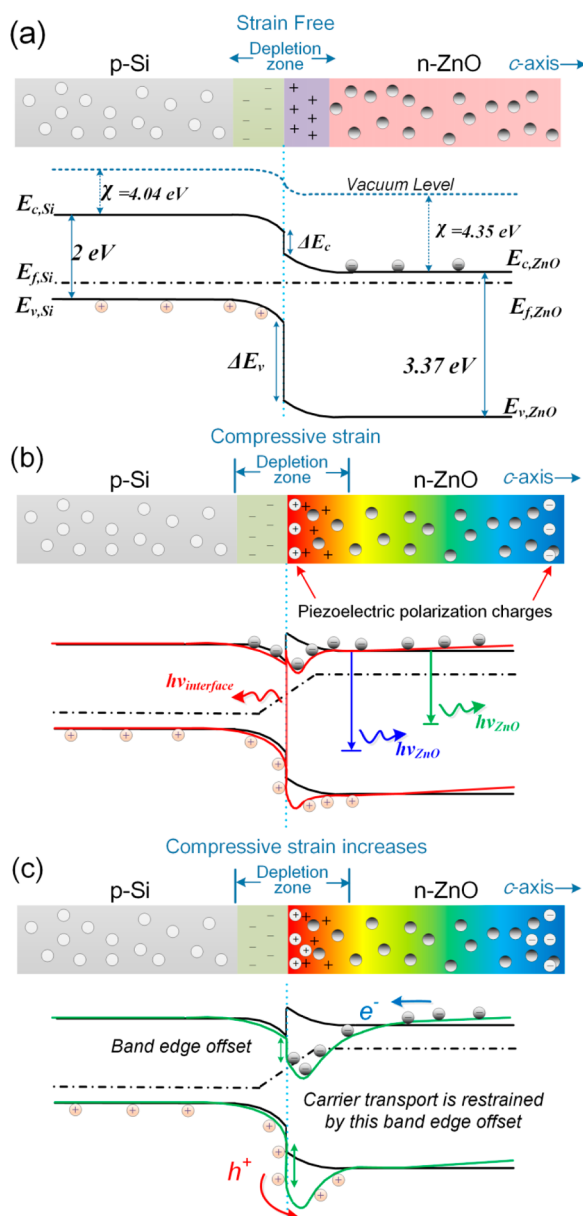


**Figure 4.** Mechanism of piezo-phototronic effect on the light intensity modulation process. (a) Band diagram of the p-Si micropillar/n-ZnO heterojunction LED device without biased voltage.  $\Delta E_c = 0.31$  eV,  $\Delta E_v = 1.68$  eV. (b) Band diagrams under forward-biased voltage (black line), where the three emission bands comprising white light are specifically indicated in different colors. When compressive strains applied, the piezoelectric polarization charges presented at the interface will introduce a dip/deformation at the conduction band edge (red line). For the color gradient, red represents positive potential and blue represents negative potential. (c) When the compressive strain keeps increasing, the deformation at the conduction band edge will make an offset (p-Si side is higher than n-ZnO side); this offset restrains the transport of electrons.

procedures.<sup>26</sup> Together with early research findings, it is proved that white light emission in Si/ZnO system is based on the size of the contact area.<sup>27</sup> It provides a promising method to manipulate the light emissions of LEDs based on piezoelectric semiconductors by the piezo-phototronic effect through applying static strains, and can be connected to other interfacial effects and lead to other possible phenomena and applications.

## METHODS

**General Fabrication Process of a SZHM Device on Microstructured Substrate.** First, the micropillar structures on the Si substrate are fabricated through photolithography and inductively coupled plasma (ICP). Second, the LED device is fabricated.

**Fabrication Process of Si Micropillar.** The P-type Si wafer was cleaned with acetone/propanol, dried under nitrogen blow, and then the Si wafer was immersed in hydrofluoric acid (HF) (1%) for 2 min. A 60 nm thick SiO<sub>2</sub> layer and a 100 nm Al layer were then grown on the wafer. Second, 50 nm thick Si<sub>3</sub>N<sub>4</sub> was deposited by plasma enhanced chemical vapor deposition (PECVD, SENTECH SI500D), and the patterned photoresist layer was fabricated through photolithography. The following step utilized inductively coupled plasma (ICP) reactive ion etching (ULVAC NE-S50H) to etch Al mask, Cl<sub>2</sub>:BCl<sub>3</sub> = 10 sccm:20 sccm, and to etch Si wafer, O<sub>2</sub>:CF<sub>4</sub>:HBr = 2 sccm:3 sccm:97 sccm. Finally, the wafer with ordered micropillars on the surface was washed with Al-11 aluminum etchant (H<sub>3</sub>PO<sub>4</sub>:CH<sub>3</sub>COOH:HNO<sub>3</sub>:H<sub>2</sub>O = 72:3:3:22), deionized water, and HF (1%) to remove the remnant Al and SiO<sub>2</sub>.

**Fabrication of Devices.** A seed layer was deposited by magnetron sputtering at 100 W for 15 min to cover the surface of the microstructured silicon wafer. In order to wrap around the silicon micropillars, a relatively thick layer of SU8 photoresist was spin-coated. The top part of the SU8 photoresist was then etched away through oxygen plasma, exposing the tips of the ZnO seed layer on the pillars. Subsequently, ZnO nanowires were grown through low-temperature hydrothermal methods. Another SU8 layer was space-filled among the clusters of ZnO nanowires. Together with plasma etching, only tips of the upright nanowires were exposed, making an ordered silicon pillar/ZnO nanowires heterojunction array. Finally, an Au layer was sputtered to form a common electrode on top of the exposed ZnO nanowires.

**Characterization and Measurement.** The Si/ZnO LED array was characterized by HRTEM (high-resolution transmission electron microscopy) (FEI Tecnai G20) and FESEM (field-emission scanning electron microscopy) (Hitachi SU8020). The Si/ZnO LED array was lit by a Maynuo DC Source Meter M8812. The CCD images were taken by test platform based on Zeiss Observer Z1. The emission spectra were obtained by spectrometer EI/FLS980. *I*-*V* characteristics were obtained by KEITHLEY 4200SCS.

## ASSOCIATED CONTENT

### Supporting Information

The Supporting Information is available free of charge on the ACS Publications website at DOI: 10.1021/acsnano.6b01666.

Figures S1–S4 showing the fabrication process, experimental setup, eight points for observing the piezo-phototronic affect, and repeatability tests (PDF)

## AUTHOR INFORMATION

### Corresponding Authors

\*E-mail: cfpan@binn.cas.cn.

\*E-mail: zlwang@gatech.edu.

### Notes

The authors declare no competing financial interest.

## ACKNOWLEDGMENTS

We are thankful for support from the “Thousand Talents” program of China for pioneering researchers and innovative teams, the President Funding of the Chinese Academy of Sciences, National Natural Science Foundation of China (Nos. 51432005, 5151101243, 51561145021, 61405040, 61505010, and 51502018), and the Beijing City Committee of Science and Technology (No. Z151100003315010).

## REFERENCES

- (1) Wu, W. Z.; Pan, C. F.; Zhang, Y.; Wen, X. N.; Wang, Z. L. Piezotronics and Piezo-Phototronics - From Single Nanodevices to Array of Devices and Then to Integrated Functional System. *Nano Today* **2013**, *8*, 619–642.
- (2) Espinosa, H. D.; Bernal, R. A.; Minary-Jolandan, M. A Review of Mechanical and Electromechanical Properties of Piezoelectric Nanowires. *Adv. Mater.* **2012**, *24*, 4656–4675.
- (3) Zhang, Y.; Liu, Y.; Wang, Z. L. Fundamental Theory of Piezotronics. *Adv. Mater.* **2011**, *23*, 3004–3013.
- (4) Pan, C. F.; Dong, L.; Zhu, G.; Niu, S. M.; Yu, R. M.; Yang, Q.; Liu, Y.; Wang, Z. L. High-Resolution Electroluminescent Imaging of Pressure Distribution Using a Piezoelectric Nanowire LED Array. *Nat. Photonics* **2013**, *7*, 752–758.
- (5) Han, X.; Du, W.; Yu, R.; Pan, C.; Wang, Z. L. Piezo-Phototronic Enhanced UV Sensing Based on a Nanowire Photodetector Array. *Adv. Mater.* **2015**, *27*, 7963–7969.
- (6) Chen, L.; Xue, F.; Li, X.; Huang, X.; Wang, L.; Kou, J.; Wang, Z. L. Strain-Gated Field Effect Transistor of a MoS<sub>2</sub>-ZnO 2D-1D Hybrid Structure. *ACS Nano* **2016**, *10* (1), 1546–1551.
- (7) Dong, L.; Niu, S.; Pan, C.; Yu, R.; Zhang, Y.; Wang, Z. L. Piezo-Phototronic Effect of CdSe Nanowires. *Adv. Mater.* **2012**, *24*, 5470–5475.
- (8) Wang, X.; Zhang, H.; Yu, R.; Dong, L.; Peng, D.; Zhang, A.; Zhang, Y.; Liu, H.; Pan, C.; Wang, Z. L. Dynamic Pressure Mapping of Personalized Handwriting by a Flexible Sensor Matrix Based on the Mechanoluminescence Process. *Adv. Mater.* **2015**, *27*, 2324–2331.
- (9) Wang, X.; Dong, L.; Zhang, H.; Yu, R.; Pan, C.; Wang, Z. L. Recent Progress in Electronic Skin. *Adv. Sci.* **2015**, DOI: [10.1002/advs.201500169](https://doi.org/10.1002/advs.201500169).
- (10) Wang, Z.; Yu, R.; Wen, X.; Liu, Y.; Pan, C.; Wu, W.; Wang, Z. L. Optimizing Performance of Silicon-Based p-n Junction Photodetectors by the Piezo-Phototronic Effect. *ACS Nano* **2014**, *8*, 12866–12873.
- (11) Xu, S.; Xu, C.; Liu, Y.; Hu, Y. F.; Yang, R. S.; Yang, Q.; Ryou, J. H.; Kim, H. J.; Lochner, Z.; Choi, S.; Dupuis, R.; Wang, Z. L. Ordered Nanowire Array Blue/Near-UV Light Emitting Diodes. *Adv. Mater.* **2010**, *22*, 4749–4753.
- (12) Wang, Z. L.; Song, J. Piezoelectric Nanogenerators Based on Zinc Oxide Nanowire Arrays. *Science* **2006**, *312*, 242–246.
- (13) Yang, Q.; Wang, W.; Xu, S.; Wang, Z. L. Enhancing Light Emission of ZnO Microwire-Based Diodes by Piezo-Phototronic Effect. *Nano Lett.* **2011**, *11*, 4012–4017.
- (14) Yang, Q.; Liu, Y.; Pan, C.; Chen, J.; Wen, X.; Wang, Z. L. Largely Enhanced Efficiency in ZnO Nanowire/p-Polymer Hybridized Inorganic/Organic Ultraviolet Light-Emitting Diode by Piezo-Phototronic Effect. *Nano Lett.* **2013**, *13*, 607–613.
- (15) Yang, Q.; Guo, X.; Wang, W.; Zhang, Y.; Xu, S.; Lien, D. H.; Wang, Z. L. Enhancing Sensitivity of a Single ZnO Micro-/Nanowire Photodetector by Piezo-Phototronic Effect. *ACS Nano* **2010**, *4*, 6285–6291.
- (16) Zhang, Y.; Gao, G.; Chan, H. L. W.; Dai, J.; Wang, Y.; Hao, J. Piezo-Phototronic Effect-Induced Dual-Mode Light and Ultrasound Emissions from ZnS:Mn/PMN-PT Thin-Film Structures. *Adv. Mater.* **2012**, *24*, 1729–1735.
- (17) Pan, C.; Chen, M.; Yu, R.; Yang, Q.; Hu, Y.; Zhang, Y.; Wang, Z. L. Progress in Piezo-Phototronic-Effect-Enhanced Light-Emitting Diodes and Pressure Imaging. *Adv. Mater.* **2016**, *28*, 1535–1552.
- (18) Guo, W.; Xu, C.; Zhu, G.; Pan, C.; Lin, C.; Wang, Z. L. Optical-Fiber/TiO<sub>2</sub>-Nanowire-Arrays Hybrid Structures with Tubular Counter-electrode for Dye-Sensitized Solar Cell. *Nano Energy* **2012**, *1*, 176–182.
- (19) Chan, Y. F.; Su, W.; Zhang, C. X.; Wu, Z. L.; Tang, Y.; Sun, X. Q.; Xu, H. J. Electroluminescence from ZnO-Nanofilm/Si-Micropillar Heterostructure Arrays. *Opt. Express* **2012**, *20*, 24280–24287.
- (20) Bao, J.; Zimmler, M. A.; Capasso, F.; Wang, X.; Ren, Z. F. Broadband ZnO Single-Nanowire Light-Emitting Diode. *Nano Lett.* **2006**, *6*, 1719–1722.
- (21) Jeong, I.-S.; Kim, J. H.; Im, S. Ultraviolet-Enhanced Photodiode Employing n-ZnO/p-Si Structure. *Appl. Phys. Lett.* **2003**, *83*, 2946–2948.
- (22) Dimova-Malinovska, D.; Nikolaeva, M. Transport Mechanisms and Energy Band Diagram in ZnO/Porous Si light-Emitting Diodes. *Vacuum* **2002**, *69*, 227–231.
- (23) Pavesi, L.; Dal Negro, L.; Mazzoleni, C.; Franzo, G.; Priolo, F. Optical Gain in Silicon Nanocrystals. *Nature* **2000**, *408*, 440–444.
- (24) Han, C. B.; He, C.; Meng, X. B.; Wan, Y. R.; Tian, Y. T.; Zhang, Y. J.; Li, X. J. Effect of Annealing Treatment on Electroluminescence from GaN/Si Nanoheterostructure Array. *Opt. Express* **2012**, *20*, 5636–5643.
- (25) Liu, Y.; Niu, S. M.; Yang, Q.; Klein, B. D. B.; Zhou, Y. S.; Wang, Z. L. Theoretical Study of Piezo-Phototronic Nano-LEDs. *Adv. Mater.* **2014**, *26*, 7209–7216.
- (26) Pan, C.; Luo, Z.; Xu, C.; Luo, J.; Liang, R.; Zhu, G.; Wu, W.; Guo, W.; Yan, X.; Xu, J.; Wang, Z. L.; Zhu, J. Wafer-Scale High-Throughput Ordered Arrays of Si and Coaxial Si/Si<sub>1-x</sub>Gex Wires: Fabrication, Characterization, and Photovoltaic Application. *ACS Nano* **2011**, *5*, 6629–6636.
- (27) Cullis, A. G.; Canham, L. T. Visible Light Emission due to Quantum Size Effects in Highly Porous Crystalline Silicon. *Nature* **1991**, *353*, 335–338.